Escola de Primavera de Transição e Turbulência
Blumenau 2020

ABCM Associação Brasileira de Engenharia e Ciências Mecânicas

12th Spring School on Transition and Turbulence
September 21st-25th, 2020, Blumenau, SC, Brazil

EPTT-2020-0072
ON THE RECEPTIVITY OF ACOUSTIC WAVES OVER LOCALIZED ROUGHNESS IN COMPRESSIBLE BOUNDARY LAYERS

Pedro Henrique Rosa dos Santos[1]
Marlon Sproesser Mathias[2]
Fernando H. T. Himeno[3]
Marcello Augusto Faraco de Medeiros[4]
[1,2,3,4] São Carlos School of Engineering, University of São Paulo, USP.
[1]pedrorosasantos@usp.br,[4]marcello@sc.usp.br

Abstract. *Surface imperfections, such as roughness, can affect laminar-turbulent transition process in boundary layers. One main engineering objective is predicting the initial amplitude of instability waves, which is a function of the flow's receptivity to external disturbances. Existing theories about receptivity are limited to restricted flow regimes and semi-empirical relations are commonly used in industry. In this scenario, this work seeks to obtain data about the receptivity of one-dimensional acoustic waves on roughness located in a flat plate boundary layer from direct numerical simulation of the Navier-Stokes equations, and extended the analysis to a compressible and non linear flow regime. To do so, a sinusoidal velocity perturbation is superimposed on the contour of the base flow. A technique based on a vanishing two-dimensional roughness is applied in order to obtain the instability waves amplitude. The data obtained will be validated with the data from recent experiments which used the same technique.*

Keywords: *Receptivity, Laminar-Turbulent Transition, DNS, Tollmien-Schlichting waves*

1. INTRODUCTION

The presence of turbulence in boundary layers affects the net drag force on vehicles, which in turn contributes to the fuel consumption and pollutant emissions. One must rely on information about the process which leads to the transition from laminar to turbulent flow to optimize the design for energetic efficiency. According to Reed *et al.* (1996), the receptivity of external disturbances to the boundary layer is substantial as it defines the initial amplitude of the instability waves, which may amplify and trigger the transition. Surface imperfections, such as isolated roughness, can provoke premature transition.

Calculation of receptivity can be found on Ruban (1984), which utilizes asymptotic expansion, and on Crouch (1992), which utilizes a finite Reynolds number theory. Both of them utilize an incompressible set of governing equations, and they are best suited for first branch receptivity, not second branch. With few exceptions, previous works in the literature often relied on this incompressible approximation.

More recent studies started investigating the influence of compressibility on the stability and receptivity, among other parameters. The work of De Tullio and Ruban (2015) presents a Direct Numerical Simulation (DNS) of the receptivity of several flow conditions to acoustic incidence on a localized bump of a gaussian shape, whose height, h, is less than 0,01% of the displacement thickness of the undisturbed boundary layer at the roughness position, δ_b^*. They compared the results from the asymptotic prediction, and they found agreement of the order of 10%. They also extended the analysis to different roughness height and found that at about $h = 0.17\delta_b^*$ the receptivity becomes nonlinear, which is in agreement with Crouch (1992), and this height is independent of Reynolds number. However, the scheme utilized has a linearization technique, and may not be fully extensible to the nonlinear regime.

The study of Raposo *et al.* (2019) made use of Adjoint Harmonic Linearised Navier Stokes Equations (AHLNS) to solve the localized roughness acoustic receptivity problem, and also utilized asymptotic expansion theory, as well as the work of De Tullio and Ruban (2015), as a benchmark. Their methodology showed remarkable accuracy and computational efficiency, yet it does not handle other flow configurations. They reported a strong dependence on Mach number, roughness streamwise position and acoustic non dimensional frequency, $F = (2\pi f_{exc}\nu)/U_\infty^2$, on the receptivity. In this equation, f_{exc} is the dimensional frequency in Hertz, ν is the kinematic viscosity and U_∞ is the free stream velocity. The difference of the receptivity between a localized roughness at the first branch in a flow with Mach number 0.1 and 0.5, both with $F = 20 \times 10^{-6}$, changed by a factor of 2.2, approximately.

Experimental works in receptivity have used a variety of approaches to measure the instability wave due to acoustic

incidence on roughness, and each of them has limitations either on the robustness, accuracy, or acquisition procedure. Placidi *et al.* (2020) presents a novel technique base on a vanishing 2D roughness to bypass some of these limitations. Its results showed a departure from the linear regime at about $h > 0.126\delta_b^*$, which is still in line with previous work, even though it has different parameters.

With the above said, the research on the compressibility effects in receptivity and its non-linear behavior is recent. In this scenario, this work has the objective of performing numerical simulations to obtain additional data about the receptivity of acoustic disturbance over localized roughness on the boundary layer and compare it with the experimental results from Placidi *et al.* (2020).

2. PROBLEM FORMULATION

The computational model used is shown in Fig 1. The red line on the left is the inflow boundary. The green line on top is the upper flow boundary. The blue line on the right is the outflow boundary. The orange line on the bottom is the free slip boundary. The black line and the rectangle on the bottom are the wall and the hump, respectively. L is the distance from leading edge to the center of the roughness, h is the height of the hump and w is the width of the hump.

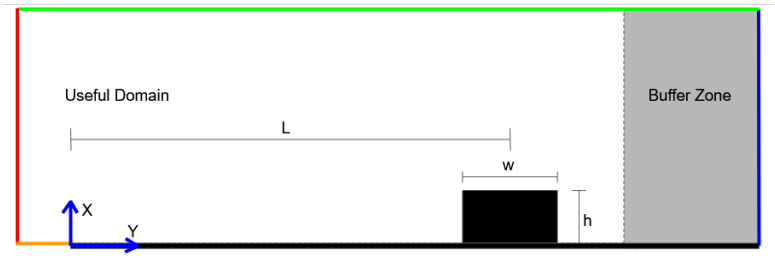

Figure 1. Computational model utilized in simulations.

The relevant flow parameters are summarized in Tab. 1. It reports the following non-dimensional numbers: $Re_\infty = U_\infty h/\nu$, $Re_h = U(h)h/\nu$, $Re_{\delta_b^*} = U_\infty \delta_b^*/\nu$ and $h^+ = hu_\tau/\nu$. These numbers are the Reynolds number based on the free stream velocity, the Reynolds number based on the velocity at roughness height, $U(h)$, the Reynolds number based on the displacement thickness of the undisturbed blasius' profile at the center of the roughness, δ_b^*, and the roughness height in wall-units, respectively.

Table 1. Flow parameters.

	h^+	Re_∞	Re_h	$Re_{\delta_b^*}$	Ma	$F \times 10^6$	h/δ_b^*	w/h
Case 1	3.6	178.1	13.2	1415.5	0.3	25	12.60%	133.3
Case 2	3.6	178.1	13.2	1415.5	0.15	25	12.60%	133.3

3. NUMERICAL SCHEME

Equations 1 to 3 presents the Compressible Navier-Stokes Equations that are directly solved via finite difference method with explicit fourth-order Runge-Kutta time marching scheme. The primitive variables are evaluated at each node in dimensionless form. In these equations, which are in index notation, ρ is specific mass, t is time, u_i is the velocity at the x_i direction, p is pressure, τ_{ij} is shear stress, e is internal energy, q_i is heat flux in the x_i direction.

$$\frac{\partial \rho}{\partial t} = -\rho \frac{\partial u_i}{\partial x_i} - \frac{\partial \rho}{\partial x_i} u_i \tag{1}$$

$$\frac{\partial u_j}{\partial t} = -\frac{\partial u_j}{\partial x_i} u_i - \frac{1}{\rho}\frac{\partial p}{\partial x_j} + \frac{1}{\rho}\frac{\partial \tau_{ij}}{\partial x_i} \tag{2}$$

$$\frac{\partial e}{\partial t} = -\frac{\partial e}{\partial x_i} u_i - \frac{p}{\rho}\frac{\partial u_i}{\partial x_i} - \frac{1}{\rho}\frac{\partial q_i}{\partial x_i} \tag{3}$$

The code uses structured mesh in a rectangular domain. There is stretching in both X and Y direction at predefined attractions points. It is possible to control the strength and size of the stretching. Care is taken to slightly modify the node position to match the roughness edges. The grid is much finer close to the wall and roughness.

Both the flat plate and the roughness walls have no-slip and no-penetration boundary conditions, as well as zero pressure gradient in the normal direction and constant temperature. Just upstream of the flat plate, there is a free-slip

region to represent free flow before the leading edge of the no-slip wall, which allows the pressure gradients just before the boundary layer to be computed correctly. The upper boundary has a Neumann boundary condition. In the outflow, the second derivatives are set to zero, except for the pressure. The pressure is defined with Dirichlet boundary condition in outflow boundary condition and Neumann in the inflow boundary condition. The pressure in both roughness' corners nodes is set to the mean of the pressures that meet the boundary condition for each direction.

A buffer zone downstream exists so oscillations are neither reflected nor amplified. It is a non-physical region where the node spacing is increased, the spatial derivative has a decreased order and there is a selective frequency damping low-pass filter (Åkervik *et al.* (2006)). To attenuate high-frequency noise, numerical low-pass filters are implemented in the domain and buffer zone (Gaitonde and Visbal (1998)) and are turned off few nodes from boundary due to large derivatives present and to avoid using uncentered stencils (Mathias and Medeiros (2018)).

The finite difference scheme has fourth-order spectral-like accuracy from Lele (1992), its stencil is five-node long and a tridiagonal system has to be solved (Martinez and Medeiros (2016)). The spatial derivatives are of a sixth-order spectral like accuracy.

To obtain the instability wave field, firstly two base flows are calculated: one with and other without roughness. Then, a sinusoidal wave is superimposed in the streamwise velocity at the inflow. It has an amplitude of $10^{-3} \times U_\infty$, where U_∞ is the reference far-field velocity. It is consistent with the disturbance amplitude measured by Placidi *et al.* (2020).

4. RESULTS

The validation of the simulation is firstly done by comparing its results against itself by changing the mesh and also by comparing it with previous works' parameters. Then, its results are compared to the data presented at Placidi *et al.* (2020). The velocity disturbance field from acoustic perturbation over the flat plate with and without roughness is presented in Fig. 2. The difference between these disturbance fields is presented in Fig. 3a, whose shape resembles a Tollmien-Schlichting (TS) wave. Figure 3b presents the density disturbance filed.

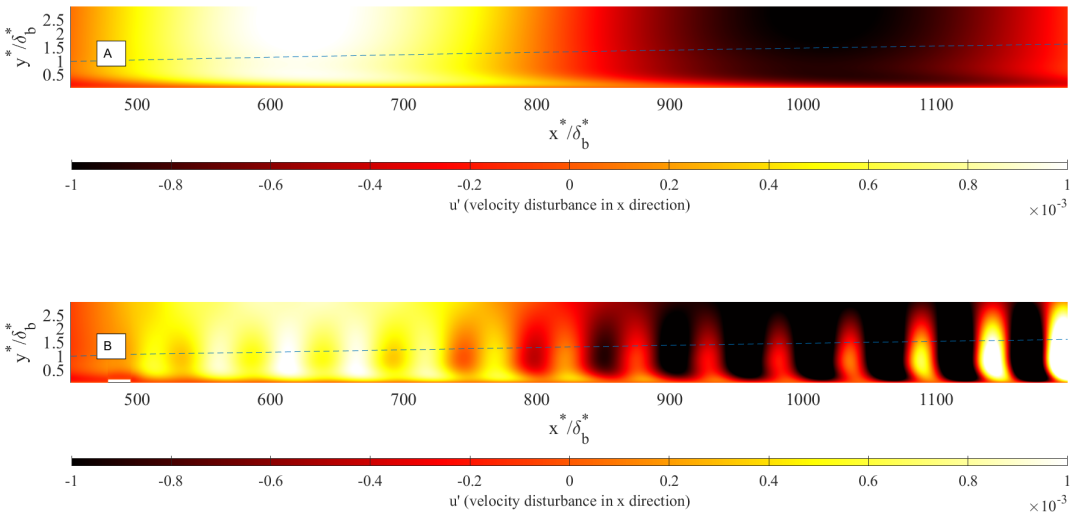

Figure 2. Contour plot of velocity disturbance on basic flow due to sinusoidal velocity wave incidence at inflow in a selected time. The dashed line in both figures are the displacement thickness of the basic flow. The figure A is the smooth flat plat and the figure B is the flat plate with localized hump. x^* and y^* are the dimensional lengths

4.1 MESH CONVERGENCE AND VALIDATION

The simulations have 12 λ_{TS} (TS wavelength) as buffer zone length, which is equivalent to 0.8 acoustic wavelengths. Also, they have a minimum of 35 points per λ_{TS} in the X direction, and 16 points in the Y direction at roughness height. The useful domain has the size of $40\delta_b^* \times 1300\delta_b^*$. A test case with a free slip boundary condition through all the flat plat without roughness was simulated with the superimposed acoustic wave. The disturbance amplitude decayed less than 0,9% from the leading edge to the roughness position. The mesh convergence study focused on the refinement over the roughness in the X-direction. One has 228 points per λ_{TS}, and the other has 425, both at roughness. The ratio between the spacing in X and Y direction for these cases are $\Delta X/\Delta Y = 27,7$ and $14,9$, respectively. The influence of Mach

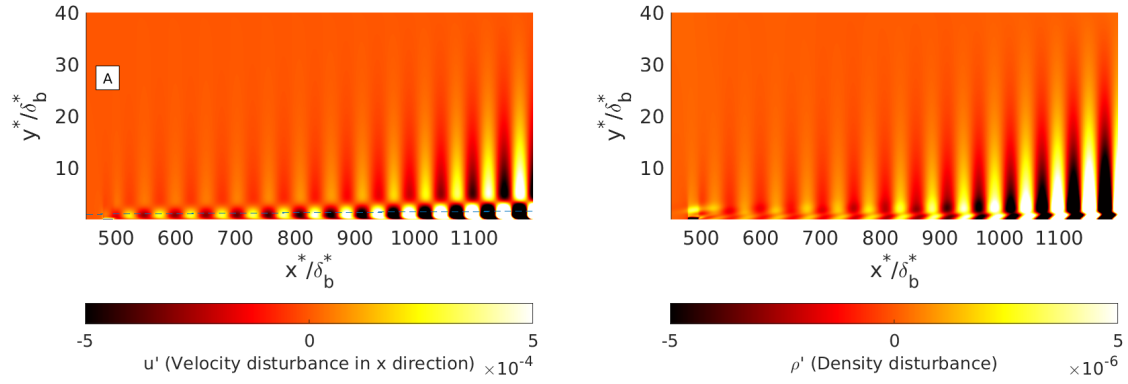

Figure 3. Instability wave. The figure on the left, A, is the velocity disturbance field, and the figure on the right, B, is the density disturbance field.

number was also investigated, and two cases with $Ma = 0.3$ and 0.15 are compared. The data presented in Placidi *et al.* (2020) are the TS amplitude in one station downstream of the roughness, and the comparison is presented in Fig. 4, which also suggests the mesh independence in the spacing in the X direction at roughness.

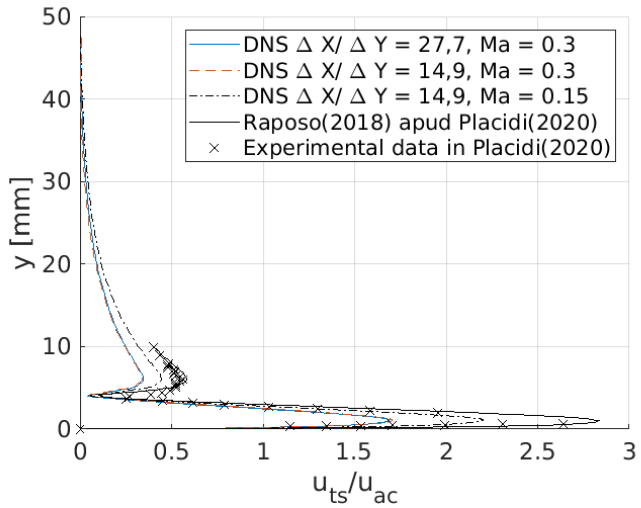

Figure 4. Instability wave amplitude at $x^*/\delta_b^* = 1106$. Comparison between this study's DNS and results in Placidi *et al.* (2020).

The difference between the experimental amplitude and the simulated one was expected since the Mach number differs. The experiment has about $Ma = 0.053$ and this study utilized $Ma = 0.3$ and $Ma = 0.15$ in order to speed up the simulation. Following the results from Raposo *et al.* (2019), the receptivity may change by a factor of order of 2 between the $Ma = 0.3$ and $Ma = 0.15$. Moreover, the TS amplification showed also a dependence on Mach number (Fig. 5).

5. DISCUSSION AND NEXT STEPS

The receptivity problem was studied with a DNS simulation and its results was compared with experimental results. Besides its effectiveness and usefulness in calculating compressible flow dynamics, the simulation can be expanded to a non-linear receptivity regime by increasing the roughness height or the acoustic wave amplitude.

Although the results seem to be in the right direction, the validation study has to be improved. It is necessary to change the Mach number, and also minimize the spurious wave reflections that yet exists. It is also necessary to investigate the domain and Y mesh independence. In the future, the DNS can simulate other types of disturbances, such as gaussian acoustic input.

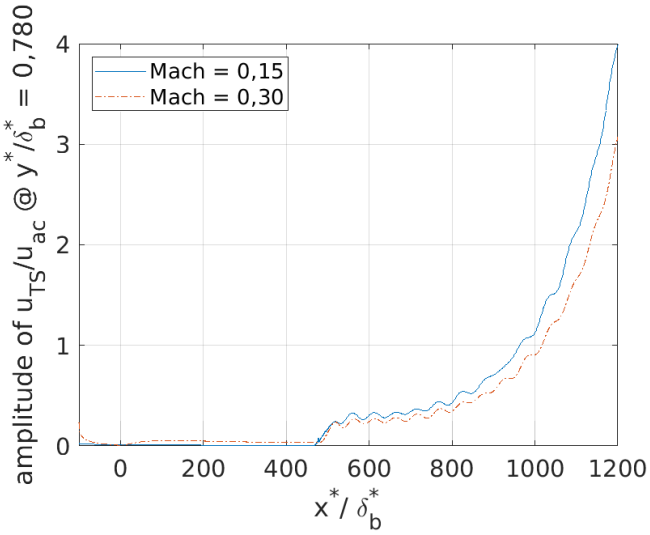

Figure 5. Instability wave amplitude at different mach numbers at a height corresponding to the maximum amplitude.

6. ACKNOWLEDGEMENTS

This study was financed in part by the Coordenação de Aperfeiçoamento de Pessoal de Nível Superior – Brasil (CAPES) – Finance Code 001. P.H.R.S is sponsored by Coordenação de Aperfeiçoamento de Pessoal de Nível Superior – Brasil (CAPES) grant no. 88882.379188/2019-01. M.S.M. is sponsored by Sao Paulo Research Foundation (FAPESP/Brazil) grant no. 2018/04584-0. F.H.T.H is sponsored by Sao Paulo Research Foundation (FAPESP/Brazil) grant no. 2018/02542-9. M.A.F.M. is sponsored by National Council for Scientific and Technological Development (CNPq/Brazil), grant no. 307956/2019-9 and the US Air Force Office of Scientific Research (AFOSR) for grant FA9550-18-1-0112, managed by Dr. Geoff Andersen from SOARD. The authors thank Professor Vassilios Theofilis for providing access to the Barkla cluster and CEPID FAPESP project no. 2013/07375-0 for providing Euler cluster infrastructure.

7. REFERENCES

Åkervik, E., Brandt, L., Henningson, D.S., Hœpffner, J., Marxen, O. and Schlatter, P., 2006. "Steady solutions of the Navier-Stokes equations by selective frequency damping". *Physics of Fluids*. ISSN 10706631. doi: 10.1063/1.2211705.

Crouch, J.D., 1992. "Localized receptivity of boundary layers". *Physics of Fluids A*, Vol. 4, No. 7, pp. 1408–1414. ISSN 08998213. doi:10.1063/1.858416.

De Tullio, N. and Ruban, A.I., 2015. "A numerical evaluation of the asymptotic theory of receptivity for subsonic compressible boundary layers". *Journal of Fluid Mechanics*, Vol. 771, pp. 520–546. ISSN 14697645. doi: 10.1017/jfm.2015.196.

Gaitonde, D.V. and Visbal, M.R., 1998. "High-order schemes for Navier-Stokes equations: algorithm and implementation into FDL3DI". *Air Vehicles Directorate*.

Lele, S.K., 1992. "Compact finite difference schemes with spectral-like resolution". *Journal of Computational Physics*. ISSN 10902716. doi:10.1016/0021-9991(92)90324-R.

Martinez, G.A.G. and Medeiros, M.A.F., 2016. "Direct numerical simulation of a wavepacket in a boundary layer at Mach 0.9". In *46th AIAA Fluid Dynamics Conference*. American Institute of Aeronautics and Astronautics, Reston, Virginia. ISBN 978-1-62410-436-7. doi:10.2514/6.2016-3195. URL `http://arc.aiaa.org/doi/10.2514/6.2016-3195`.

Mathias, M.S. and Medeiros, M.A.F., 2018. "Direct Numerical Simulation of a Compressible Flow and Matrix-Free Analysis of its Instabilities over an Open Cavity". *Journal of Aerospace Technology and Management*, Vol. 10. ISSN 2175-9146. doi:10.5028/jatm.v10.949. URL `http://www.jatm.com.br/ojs/index.php/jatm/article/view/949`.

Placidi, M., Gaster, M. and Atkin, C.J., 2020. "Acoustic excitation of Tollmien-Schlichting waves due to localised surface roughness". *Journal of Fluid Mechanics*, pp. 1–13. ISSN 14697645. doi:10.1017/jfm.2020.349.

Raposo, H., Mughal, S.M. and Ashworth, R., 2019. "An adjoint compressible linearised Navier-Stokes approach to model generation of Tollmien-Schlichting waves by sound". *Journal of Fluid Mechanics*, Vol. 877, pp. 105–129. ISSN 14697645. doi:10.1017/jfm.2019.601.

Reed, H.L., Saric, W.S. and Arnal, D., 1996. "Linear Stability Theory". *Annual Review of Fluid Mechanics*, Vol. 28, pp. 389–428.

Ruban, A.I., 1984. "On the generation of Tollmien-Schlichting waves by sound". *Fluid Dynamics*, Vol. 19, No. 5, pp.

709–717. ISSN 1573-8507. doi:10.1007/BF01093536. URL https://doi.org/10.1007/BF01093536.

8. RESPONSIBILITY NOTICE

The authors are the only responsible for the printed material included in this paper.